Springer

KSME

Journal of Mechanical Science and Technology 33 (9) (2019) 4217~4226
www.springerlink.com/content/1738-494x(Print)/1976-3824(Online)
DOI 10.1007/s12206-019-0817-9

Experimental and numerical characterization of mechanical properties of carbon/jute fabric reinforced epoxy hybrid composites †

Aakash Ali[1], Muhammad Ali Nasir[1,*], Muhammad Yasir Khalid[2], Saad Nauman[3], Khubab Shaker[4], Shahab Khushnood[1], Khurram Altaf[5], Muhammad Zeeshan[4] and Azhar Hussain[1]

[1]*Department of Mechanical Engineering, University of Engineering and Technology, Taxila, Pakistan*
[2]*Department of Mechanical Engineering, University of Management and Technology, Lahore, Pakistan*
[3]*Department of Material Science, Institute of Space Technology, Islamabad, Pakistan*
[4]*National Textile University, Punjab, Pakistan*
[5]*Mechanical Engineering Department, Universiti Teknologi Petronas, 32610 Bandar Seri Iskandar, Perak, Malaysia*

(Manuscript Received December 3, 2018; Revised May 28, 2019; Accepted June 19, 2019)

Abstract

Natural fiber composites have great potential for reducing the product cost, lowering weight and enhancing renewability. Functionality and performance of natural fibers can be enhanced many folds using them together with synthetic fibers. Hybridization of carbon and low-cost natural jute fiber offers a sustainable hybrid composite having high modulus and mechanical strength. This study investigates flexural behavior of carbon/jute epoxy composites experimentally and numerically. Also, impact response is characterized through drop weight method. Study concludes that flexural strength decreases with increase in jute percentage. Simulation of flexural behavior diverges more than 10 % from experimental results. This anomaly is due to waviness of fiber resulting in heterogeneous property distribution in composites. Further, the fracto-graphic study revealed modes of failure. The drop weight impact tests reveal increased damage area with increase in jute percentage.

Keywords: CFRP; Drop weight test; Flexural test ; Hybrid; Numerical simulation

1. Introduction

Fiber reinforced polymer composites are being utilized in various industries such as sports [1-3], automotive [4-6] and aerospace [7-9] because of their unique properties such as high strength to weight ratios, corrosion resistance and vibration absorption abilities as compared to metals. Laminated composites consist of several thin layers of fibers connected by a matrix. These laminated composites are generally reinforced with synthetic fibers like carbon and glass fibers. Lamination can be utilized to improve strength, stiffness, corrosion resistance, thermal insulation and moisture absorption. Synthetic fibers have high strength as compared to natural fibers but at the same time they are expensive. On the other hand natural fiber reinforcements stand out because of their low cost, biodegradability, renewability, low density and environmental friendly nature. Hybrid fiber composites are manufactured by using two or more types of reinforcements embedded in single matrix. Hybridization using natural and synthetic fiber reinforcements is an efficient way of exploiting the use of natural fibers in structural applications [6]. Combination of carbon with a low cost natural fiber such as jute offers a more sustainable structure as compared to typical carbon fiber reinforced polymer (CFRP) structure. Jute adds its damping properties whereas carbon fibers bring their mechanical properties into the hybrid composite laminates. These hybrid composites can replace CFRP in structures prone to vibrations [10]. Strength of fiber reinforced composites depend on fiber properties, properties of matrix and the interfacial interaction between matrix and the fiber. In flexural loading exterior plies bear tensile and compressive stresses while neutral axis passes through the centroid where no stresses exists. It can be hypothesized that hybrid fiber reinforced composite structures will posses higher flexural [11] and impact strength when stiffer plies are placed at the exterior [12]. In the similar vein it can be expected that with the increase in the proportion of jute fiber layers, flexural and impact strength will decrease. Moreover the natural tendency of natural fibers to absorb moisture from the environment can be minimized by placing natural fiber layers as interior plies.

Citil employed non-linear three-dimensional finite element

*Corresponding author. Tel.: +92 51 9047688
E-mail address: ali.nasir@uettaxila.edu.pk
† Recommended by Associate Editor Jin Weon Kim

method to evaluate bending response of adhesively bonded curved lap joints. Experimental tests were also conducted to validate numerical results. Experimental and numerical solutions were found to be compatible [13]. Semsettin et al. performed non-linear analysis to predict response of bi-adhesive in double strap joint provided with an embedded patch under bending load. By means of bi-adhesive failure loads were found to show the increase ratio between 9 % and 56 % [14]. Vinsova and Urban conducted a numerical study on thick-walled CFRP composites to obtain flexural properties. Both unidirectional and woven reinforcements were utilized in composites fabrication. In order to obtain elastic properties of material, thin-walled CFRP composites were fabricated and tensile tests were performed to obtain tensile modulus strength and Poisson ratio. These elastic constants obtained were used in FEM simulations of thick-walled composites. The calculation error of simulation for unidirectional fiber reinforced composites was found to be 10 % while error for woven composites was higher [15].

Chaudhary et al. evaluated flexural strength of unfilled glass fiber reinforced polymer (GFRP) composite numerically and experimentally as per ASTM D790 standard. Error between FEM simulation and experimental results was found to be in range of 10 % [16]. Bajpai et al. performed flexural tests to evaluate flexural strength of different combinations of glass/jute epoxy composites. Composite having one glass and three jute plies displayed higher flexural strength [17]. Indra Reddy et al. conducted experiments on Jute, pineapple leaf and glass fiber epoxy composites according to ASTM D790 to find flexural strength. Increase in flexural strength was observed with increasing fiber volume fraction [18].

Gupta and Singh studied polylactic acid coated sisal fiber polyester composites experimentally to find flexural properties as per ASTM D790. Study demonstrated improvement in flexural strength using PLA coating on sisal fiber composites [19].

Ullah et al. determined bending response of woven GFRP composites through simulations using ABAQUS. Internal heterogeneity of woven composites resulted in slight divergence of FEM simulation results from those of experimental [20].

Soliman et al. determined on-axis and off-axis flexural strengths of carbon woven composites experimentally and numerically. FE simulations verified fiber dominance in on-axis flexural performance while matrix govern performance in off-axis flexural strength [21].

Gruber and Wartzack performed an anisotropic simulation to analyze three-point bending response of short fiber reinforced thermoplastic and obtained results were compared with experimental results. Integrative simulation for early design steps predicted absolute displacement values precisely [22].

Rafiquzzaman et al. conducted a numerical analysis of glass/jute reinforced epoxy hybrid composite laminates and then compared numerical results with experimental results. In this study, complete model was divided into different layers of composite plates to represent different mechanical properties for each layer. Isotropic type of material was assigned to composite plates as an input in FEM simulation. Approximately, 15-20 % error was found between maximum stress values of simulation and experiment [23]. Dong et al. computed the flexural strengths of different stacking sequences of s-glass and carbon fiber reinforced epoxy hybrid laminates using classical laminate theory. Results obtained revealed validity of suggested model when compared with simulation results [24].

Different simulation options were also evaluated for GFRP rectangular composite beams consisting of two different adhesives polyurethane and epoxy [25].

Ramana and Ramprasad conducted experimental study to determine flexural strength of carbon-jute epoxy hybrid composite containing 22 % carbon, 23 % jute and 55 % epoxy. Research concluded that these hybrid composites can replace CFRP with small loss in flexural strength [26].

Abhishek et al. conducted probabilistic study of flexural strength of untreated jute reinforced polyester composites according to ASTM D7264. Maximum flexural strength was found in composites having 3.48 mm thickness and 15.62 % fiber volume fraction [27].

Braga and Magalhaes tested jute/glass epoxy hybrid composites experimentally to get flexural strength according to ASTM D790. Maximum flexural strength was found when glass plies were used at exterior [28].

Sezgin and Berkalp studied impact response of jute-carbon hybrid composites. Carbon fiber addition produced not only high tensile strength but also improved impact strength as compared to only jute composites [29]. Hung et al. performed a low velocity impact experimental analysis on different stacking sequences of glass/carbon reinforced polymer composites according to ASTM D7136. Samples containing surface carbon plies and glass plies in core presented high impact resistance in terms of local damage (delamination) while severe damage was found on samples with surface glass plies and core carbon plies [7].

Hongxiao et al. studied design optimization of CFRP stacking sequence for improving impact strength using a multi island genetic algorithms. Improved specimen was comprised of variety of angled plies as compared to base line laminate and presented 42.1 % less damage than base line laminate [30].

Sevkat et al. performed drop weight impact tests on woven hybrid composites using impactors of various geometries. glass/graphite/glass composite sustained higher impact loads while graphite/glass/graphite laminate displayed low delamination phenomenon [31].

Sarasini et al. conducted low velocity impact analysis on carbon/basalt epoxy hybrid laminates having two different combinations i.e. intercalated and sandwich-like. Post impact properties were characterized through flexural and inter laminar shear strength (ILSS) tests along with non-destructive tests: Acoustic emission and ultrasonic phased array. Higher impact energy absorption was found in intercalated sequence as compared to sandwich-like [32].

Gopinath et al. evaluated impact strength of jute fiber epoxy composites. Impact strength improved upon fiber treatment

with 5 % NaOH [33].

Ahmed et al. conducted low velocity impact damage analysis of woven jute/glass reinforced isothalic polyester composite. Jute composites demonstrated better energy absorption capacity as compared to jute/glass hybrid while jute/glass composites displayed better damage tolerance capability [34].

Sugun and Rao performed repeated drop tests on glass, carbon and kevlar composites to study low velocity impact behavior. The degree of impact damage was interpreted using delamination area maps. Results for all three laminates explored that with a rise in drop numbers, the peak load gradually lessened whereas the total energy increased, until failure [35].

Supratik et al. studied effects of material, process and test parameters on low velocity impact damage of glass-epoxy laminates. Research revealed dependency of thickness on process parameters; and for a constant energy level, the number of drops (required for material failure) were in direct relationship to laminate thickness [36].

Zhang et al. conducted drop weight impact damage analysis for woven carbon fiber reinforced epoxy composites manufactured by different processes i.e., autoclave and quick step. Optical micrography of quick step cured laminates revealed more ductility and less severe matrix damage as compared to autoclave [37].

It can be noticed that previous researchers have found that carbon-jute hybrid composites can replace carbon fiber reinforced polymer (CFRP) composites without significant loss in mechanical properties and with improved damping properties.

2. Experimental work

2.1 Materials and methods

In this study we used plain-woven carbon 3K and plain-woven jute reinforcements as shown in Figs. 1 and 2 respectively along with epoxy resin (epotec yd128). Jute was supplied by Yarn Fabric Manufacturing Department National Textile University Faisalabad. Carbon fabric was purchased from Vital Polymers, Sialkot while epoxy from Pak Welcome Trade Blue area, Islamabad.

2.2 Fabrication method

Hand layup technique was employed to fabricate hybrid composite for following experimentation. First of all, mold releasing agent was sprayed on mold surface and peel ply was placed above it which helped in gaining good surface finish and easy separation of composites from mold. Then epoxy was applied by brush on first layer of carbon. Afterwards, roller was rolled manually to get uniform distribution of epoxy on fiber surface and remove excessive epoxy as shown in Fig. 3. Similarly, desired stacking schemes, discussed in Table 1, were achieved by repeating these simple steps. Samples were manufactured on basis of layers stacking schemes and then percentage weights were calculated for each material. The specimens for mechanical testing were obtained by cutting fabricated composite plates by grinding machine. The cutting was performed according to ASTM D7264 and ASTM D7136 for flexural testing and drop weight testing, respectively.

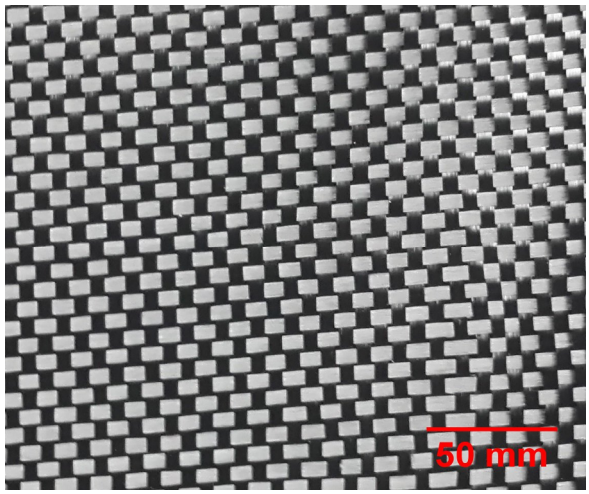

Fig. 1. Plain woven carbon fabric.

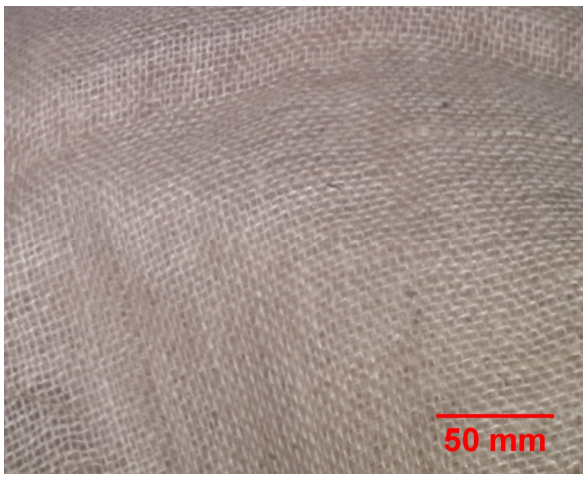

Fig. 2. Plain woven jute fabric.

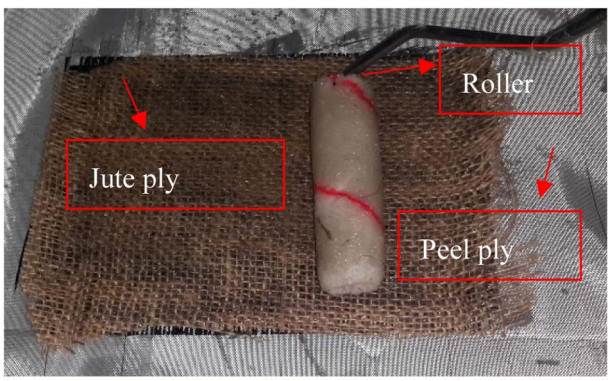

Fig. 3. Roller was used to remove excess epoxy.

Table 1. Samples schemes and their mass percentage.

Samples stacking sequence	Coding	% weight of jute	% weight of carbon	% weight of epoxy
Carbon/carbon/jute/carbon/carbon	CCJCC	8.2	33.8	57.9
Carbon/jute/carbon/jute/carbon	CJCJC	15.4	23.7	60.9
Carbon/jute/jute/jute/carbon	CJJJC	19.2	13.02	67.7

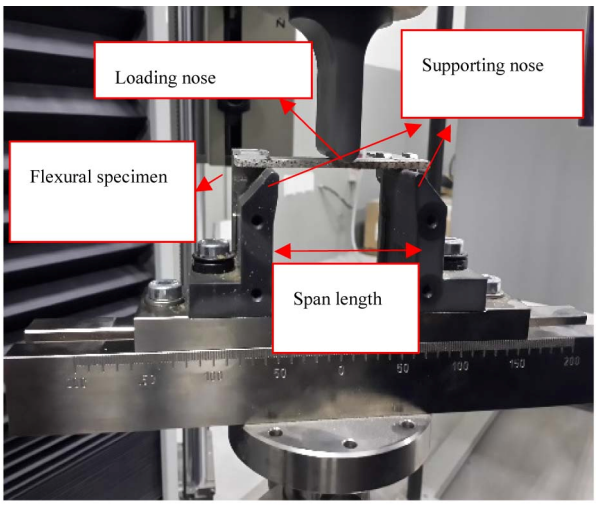

Fig. 4. Flexural specimen during test.

2.3 Mechanical testing

2.3.1 Flexural testing

Three-point bending test was performed according to ASTM D7264 [38] and thickness to span ratio was 1:20 on Zwick/Roell Z100 as displayed in Fig. 4. The thickness of specimens ranged from 1.92 mm to 2.98 mm. The strain rate was 1 mm/min at room temperature. Average results were obtained by performing experiments on three samples for each test. Further, the fractured surfaces were studied under Olympus BX51 microscope.

2.3.2 Drop weight testing

Drop weight impact testing was performed on three types of samples as per ASTM D7136 [39]. The specimen dimensions were 150 mm*100 mm and thickness was 2.2 mm as shown in Fig. 5. Impactor energy was selected at 15 Joules on Zwick Roell HIT230F as shown in Fig. 6. Specimen was clamped in jaws of machine as shown in Fig. 7.

3. Numerical analysis for flexural testing

Simulations of three-point bending tests were performed to determine the flexural strengths using ABAQUS.

In three-point bending test simulation, composite part was modelled as deformable 3D shell while discrete rigid extruded solids were used for: Support cylinders having radius of 3 mm, and loading nose having radius of 5 mm. Then, these extruded solids were converted into shell. Each ply was defined by orthotropic materials properties. Orthotropic lamina was defined by nine engineering constants as shown in Table 2.

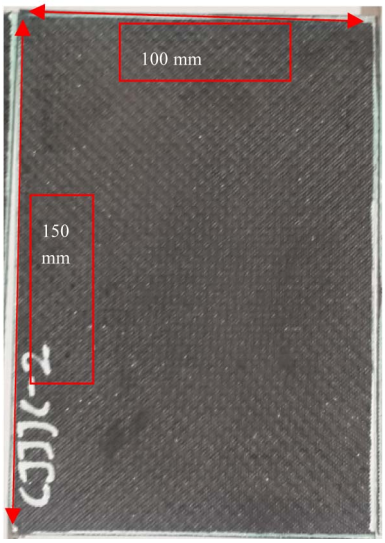

Fig. 5. Impact specimen.

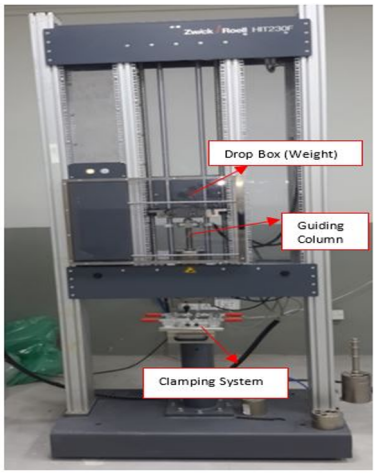

Fig. 6. Zwick Roell HIT230F machine.

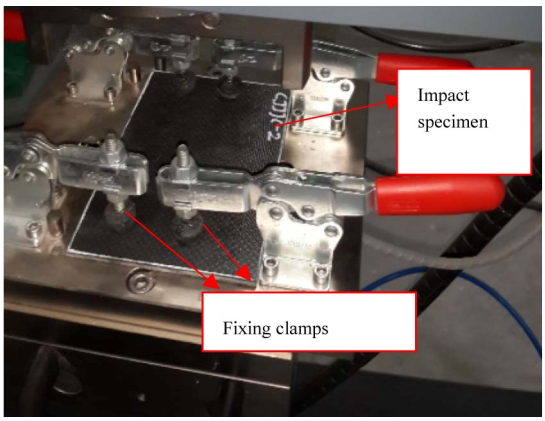

Fig. 7. Specimen clamped in jaws.

Table 2. Lamina properties for numerical simulation.

Physical property	Carbon/epoxy lamina	Jute/epoxy lamina
Density (kg/m^3)	1050.7	826.07
$E_1 = E_2$ (MPa)	40000 [40]	3400
E_3 (MPa)	5077	3200
G_{12} (MPa)	4000 [41]	1574
$G_{23} = G_{13}$ (MPa)	2277	1536
v_{12}	0.045 [41]	0.08
$v_{23} = v_{13}$	0.3	0.32

Table 3. Specimens average dimensions.

Stacking sequence	Span length (mm)	Average width (mm)	Thickness (mm)
CCJCC	40	13.86	1.92
CJCJC	52	13.46	2.56
CJJJC	58	13.88	2.98

Young modulus of carbon/epoxy ply was taken from Ref. [40]. For jute/epoxy woven ply, ply tensile test was performed, according to ASTM D3039, at a loading rate of 5 mm/min to determine E1, E2 and v12. This was to take into account weave effect as Young modulus of textile composites decreased due to waviness nature of fabric reinforcements. The correct evaluation of E1, E2 and v12 for a ply plays a great role in convergence of simulation with experimental results. G12and v12 of carbon/epoxy ply were taken from Ref. [41]. While G12 of jute/epoxy ply was obtained analytically by assuming transverse isotropy along 1 and 2 principle directions because of woven nature fiber is running along both these directions. The remaining engineering constants of both plies i.e. E3, G23, G13, v23, v13 were calculated analytically using rule of mixture (ROM).

Hybrid composites stacking sequence was defined in "composite-layup manager" by giving each ply material and thickness as discussed in Table 3. Carbon epoxy ply thickness was taken as 0.26 mm while jute epoxy ply thickness was determined by subtracting total carbon epoxy plies thickness from laminate thickness. In assembly module, dependent mesh was selected and cylinders were shifted to offset points above and below from mid-plane at a distance half of thickness of part. Reason for this offset was definite thickness associated with 3D shell element. In step module, analysis steps and type of analysis were defined and declared. Flexural analysis was declared as static general. Output requests could also be nominated in this module.

In interaction module, general contacts (standard) were defined between supports, loading nose and part with 0.15 friction coefficient in tangent direction and hard mechanical contact in normal direction. In flexural test simulation, reference points of 3 mm radius support cylinders were constrained as ENCASTRE while reference point of upper cylinder (loading nose) was displaced by displacement load. The meshed parts are shown in Fig. 8.

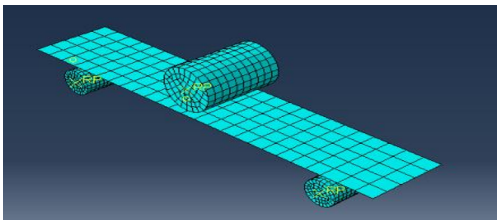

Fig. 8. Meshed parts.

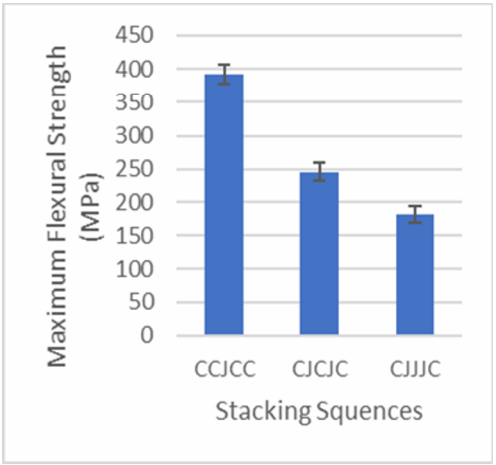

Fig. 9. Bar chart for maximum flexural strength of different sequences.

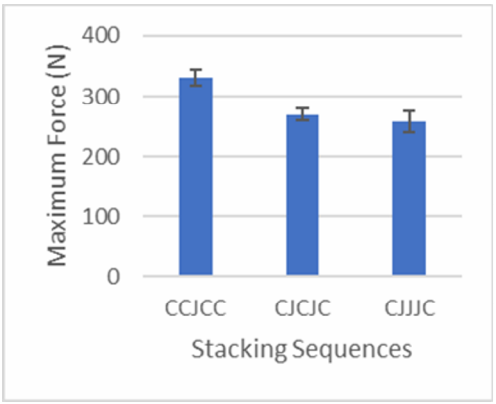

Fig. 10. Bar chart for maximum force of different sequences.

4. Results and discussion

4.1 Flexural testing

The experimental results revealed that composite containing more carbon plies at exterior possessed high flexural strength.

Bar charts for maximum flexural strength and maximum force are shown in Figs. 9 and 10, respectively.

The FEM simulations deviated more than 10 % from experimental results. This difference was due to: Non-uniform property distribution produced by waviness nature of rein-

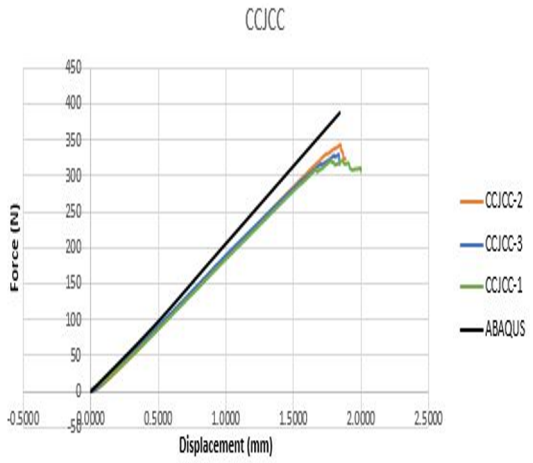

Fig. 11. Comparison of graphs of CCJCC sequence.

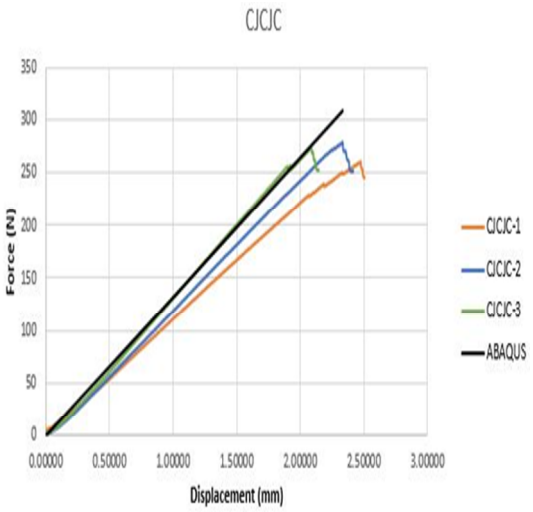

Fig. 12. Comparison of graphs of CJCJC sequence.

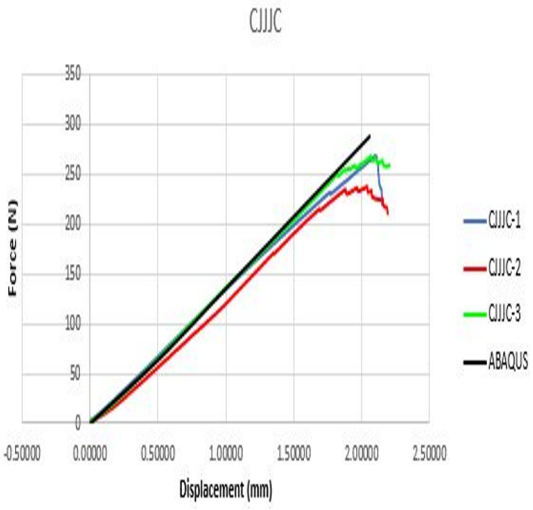

Fig. 13. Comparison of graphs of CJJJC sequence.

Table 4. Damage area for CCJCC scheme.

Scheme	Trials	Damage area (cm Sq.)	Average damage area (cm Sq.)
CCJCC	Trial-1	5.32	6.07
	Trial-2	7.45	
	Trial-3	5.46	

Table 5. Damage area for CJCJC scheme.

Scheme	Trials	Damage area (cm Sq.)	Average damage area (cm Sq.)
CJCJC	Trial-1	5.89	6.75
	Trial-2	6.36	
	Trial-3	8.02	

Table 6. Damage area for CJJJC scheme.

Scheme	Trials	Damage area (cm Sq.)	Average damage area (cm Sq.)
CJJJC	Trial-1	16.13	14.45
	Trial-2	12.67	
	Trial-3	14.56	

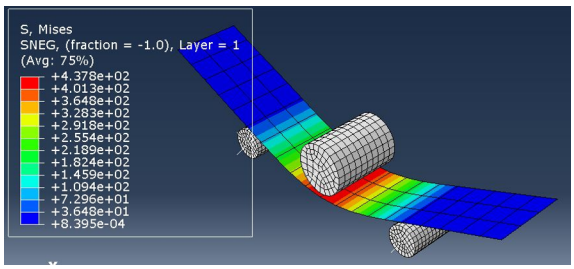

Fig. 14. Contour plots for von-Mises stresses CCJCC.

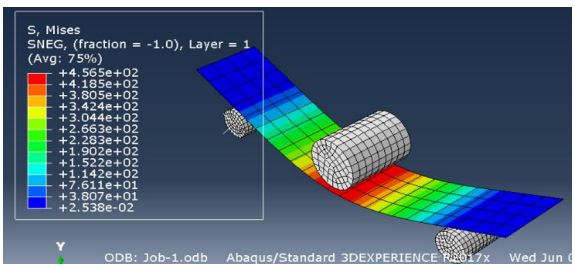

Fig. 15. Contour plots for von-Mises stresses CJCJC.

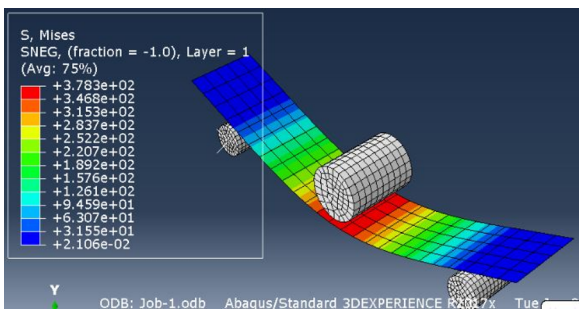

Fig. 16. Contour plots for von-Mises stresses CJJJC.

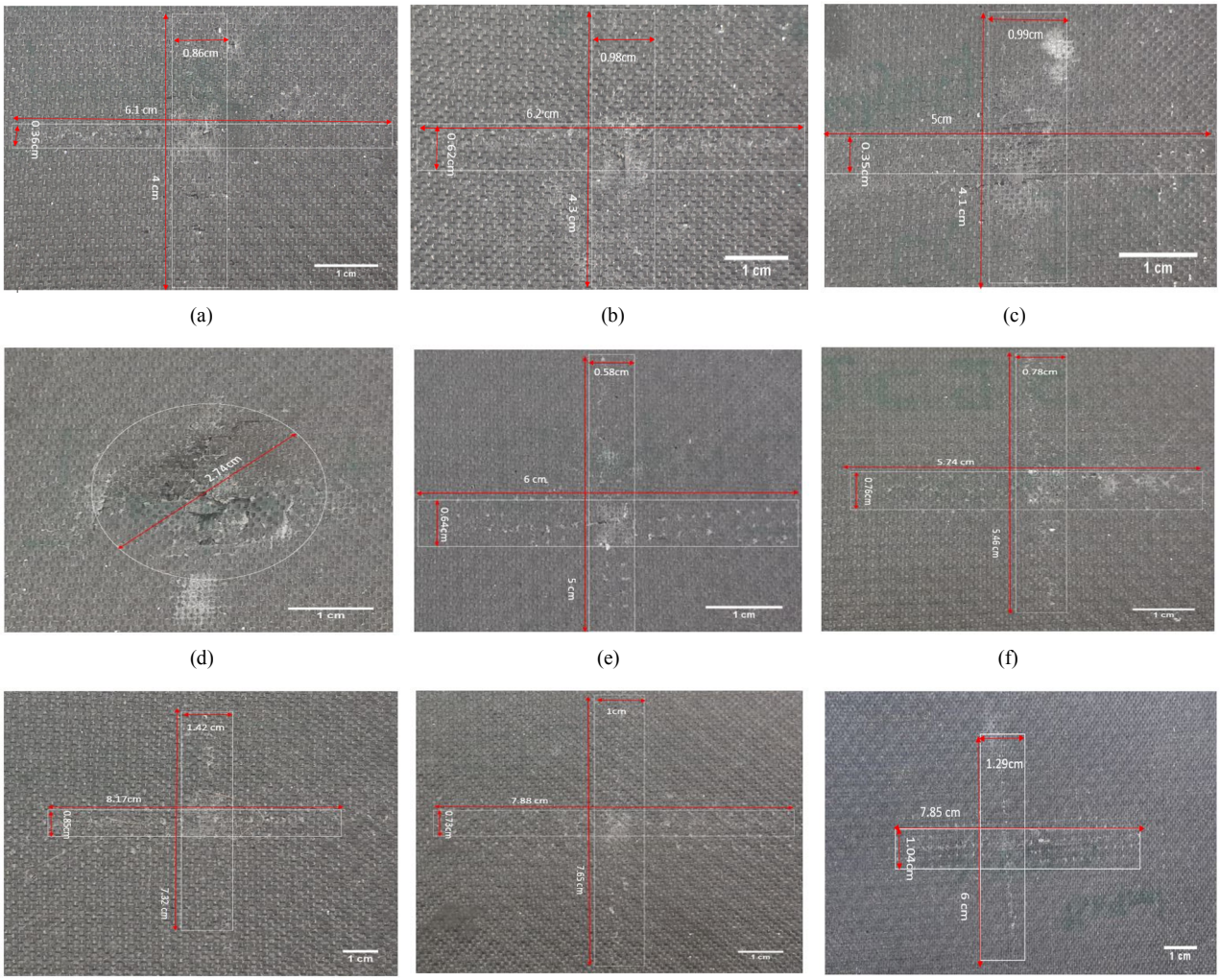

Fig. 17. CCJCC sample at different trials: (a) CCJCC sample at trial-1; (b) CCJCC sample at trial-2; (c) CCJCC sample at trial-3; (d) CJCJC sample at trial-1; (e) CJCJC sample at trial-2; (f) CJCJC sample at trial-3; (g) CJJJC sample at trial-1; (h) CJJJC sample at trial-2; (i) CJJJC sample at trial-3.

forcements, micro voids due to hand layup manufacturing process, and possibility of delamination in real experimental model. In hand layup, epoxy was dispersed manually by roller making it impossible to achieve uniform epoxy distribution.

Comparison of experimental and numerical force displacement curves is presented in Figs. 11-13. While Contour plots for different sequences are shown in Figs. 14-16.

4.2 Impact testing

The optical damaged area images of different samples are shown in Fig. 17. Furthermore, this damage area is also calculated for all samples as discussed in Tables 4-6. Damage area increased with increase in jute mass percentage and maximum damage area was found in CJJJC scheme while minimum damage area was found in CCJCC scheme. It can be observed that average damage areas found in CCJCC and CJCJC are approximately equal. Alternate sequence CJCJC (which contains more natural jute than CCJCC) can replace CCJCC in impact applications with small loss in impact damage resistance.

5. Fractographic study for flexural specimens

Fractographic study was conducted on Olympus BX51 microscope. Images of fractured specimens were observed from different views to study modes of failure. Ply touching loading nose endured compressive load while tension load appeared at ply touching supports as shown in Figs. 18 and 19, respectively.

SEM analysis figures out that fibers of top ply are buckled due to compression load as shown in Fig. 20. Matrix failure occurs in form of matrix fragmentation as shown in Fig. 21. Matrix/fiber fragmentation happens because of abrasion of the matrix from fiber fracture surfaces as a result of flexural loading. Spikes/hackles shown in Fig. 22 are revealing effective

Fig. 18. Ply failure due to compressive load.

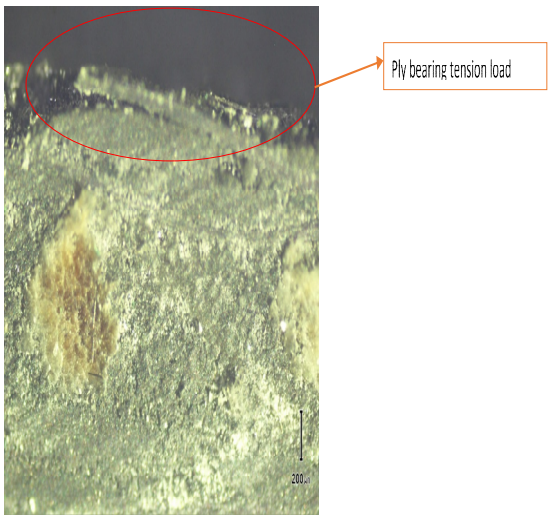

Fig. 19. Ply bearing tension load.

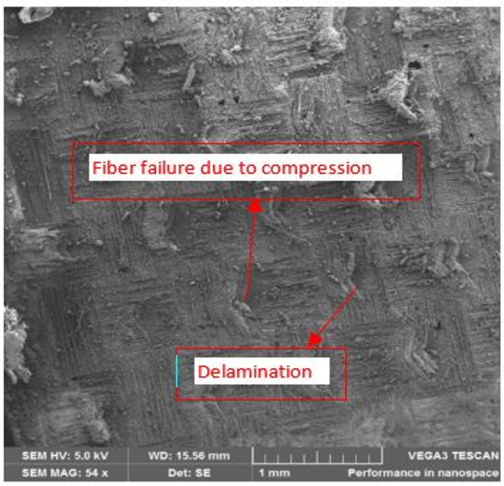

Fig. 20. Fiber failure.

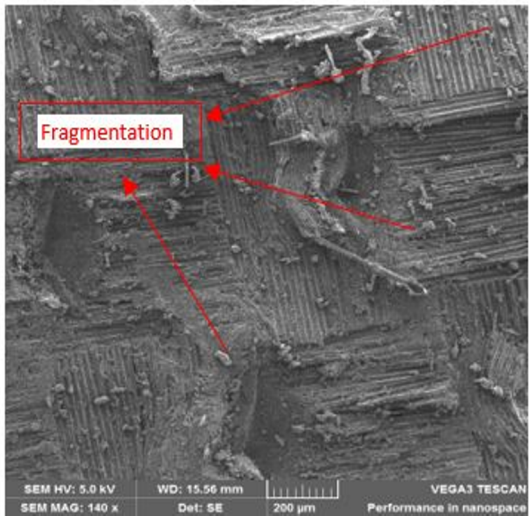

Fig. 21. Matrix failure.

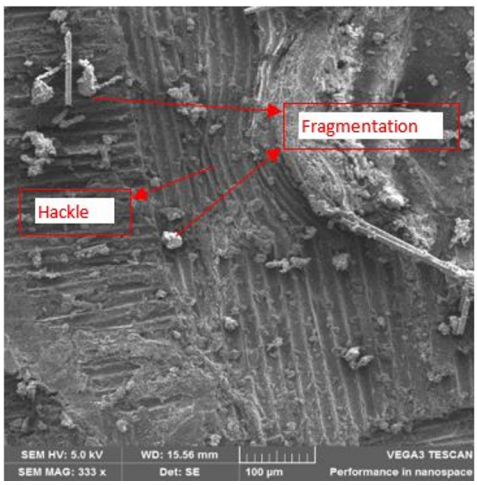

Fig. 22. Hackle and fragmentation.

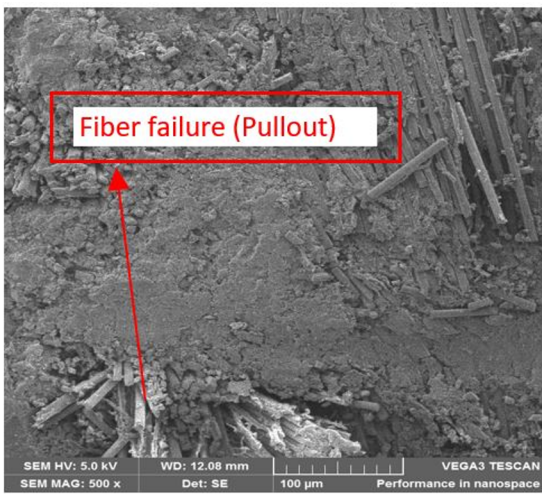

Fig. 23. Fiber pullout.

load transfer from fiber to fiber through matrices. Also, fiber pull out can be seen in Fig. 23, which occurs because of weak interfacial adhesion between fiber and matrix.

6. Conclusions

Study concluded that the specimen having more outer carbon plies i.e., CCJCC had highest flexural strength than other sequences due to high stiffness of carbon reinforcement.

Analysis of impact damage areas of different hybrid sequences figured out that impact strength decreased with decrease in carbon mass percentage. It can be concluded that CJCJC can replace CCJCC in impact applications with no significant loss in impact damage resistance. Decrease in carbon plies caused decrease in flexural strength as well as impact resistance. The results of numerical simulation of flexural tests were in good agreement with experimental results which demonstrated capability of simulation technique to predict flexural behavior. These simulations are widely used in aerospace and automotive industries for nondestructive characterization of material for design and analysis. There was slight mismatch between simulation and experimental curves due to possibility of micro voids and non-uniform epoxy distribution. These anomalies were due to hand layup technique and woven nature of reinforcements as woven composites show heterogeneous property distribution.

Fractographic study explored mode of failures i.e., compression and tension failure in top and bottom plies respectively. SEM analysis explored that fiber failure involved buckling, pullout and delamination while matrix failure occurred in form of fragmentation.

References

[1] G. H. Sun and J. J. Wang, The applied research of fiber reinforced composites materials in sports equipments, *Adv. Mater. Res.*, 485 (2012) 506-509.

[2] L. N. Sun and Z. Deng, The carbon fiber composite materials application in sports equipment, *Adv. Mater. Res.*, 341-342 (2011) 173-176.

[3] M. A. Nasir et al., Smart sensing layer for the detection of damage due to defects in a laminated composite structure, *J. Intell. Mater. Syst. Struct.*, 26 (17) (2015) 2362-2368.

[4] H. Adam, Carbon fibre in automotive applications, *Mater. Des.*, 18 (4-6) (1997) 349-355.

[5] S. Anas et al., Influence of MWCNTs as secondary reinforcement material in glass fiber / epoxy composites fabricated using VARTM, *Appl. Compos. Mater.*, 2 (1) (2013) 17-26.

[6] S. N. A. Safri, M. T. H. Sultan, M. Jawaid and K. Jayakrishna, Impact behaviour of hybrid composites for structural applications: A review, *Compos. Part B Eng.*, 133 (2018) 112-121.

[7] P. Hung, K. Lau, L. Cheng, J. Leng and D. Hui, Impact response of hybrid carbon / glass fi bre reinforced polymer composites designed for engineering applications, *Compos. Part B*, 133 (2018) 86-90.

[8] F. Sarasini et al., Drop-weight impact behaviour of woven hybrid basalt-carbon/epoxy composites, *Compos. Part B Eng.*, 59 (2014) 204-220.

[9] S. Zahid et al., Experimental analysis of ILSS of glass fibre reinforced thermoplastic and thermoset textile composites enhanced with multiwalled carbon nanotubes, *J. Mech. Sci. Technol.*, 33 (1) (2019) 197-204.

[10] S. Ashworth, J. Rongong, P. Wilson and J. Meredith, Mechanical and damping properties of resin transfer moulded jute-carbon hybrid composites, *Compos. Part B*, 105 (2016) 60-66.

[11] J. Zhang, K. Chaisombat, S. He and C. H. Wang, Hybrid composite laminates reinforced with glass/carbon woven fabrics for lightweight load bearing structures, *Mater. Des.*, 36 (2012) 75-80.

[12] N. K. Naik, R. Ramasimha, H. Arya, S. V Prabhu and N. Shamarao, Impact response and damage tolerance characteristics of glass ± carbon / epoxy hybrid composite plates, *Composites Part B: Engineering*, 32 (2001).

[13] Ş. ÇİTİl, Experimental and numerical investigation of adhesively bonded curved lap joints under three-point bending, *Mechanika*, 24 (6) (2018) 824-832.

[14] Ş. Temiz, H. Adin and I. Sülü, Behaviour of bi-adhesive in double-strap joint with embedded patch subjected to bending, *J. of Theoretical and Applied Mechanics*, 45 (2015).

[15] L. Vinšová and T. Urban, Testing of mechanical properties of thick-walled carbon fiber composite for FEM simulations, *Mater. Today Proc.*, 4 (5) (2017) 5989-5994.

[16] S. K. Chaudhary, K. K. Singh and R. Venugopal, Experimental and numerical analysis of flexural test of unfilled glass fiber reinforced polymer composite laminate, *Mater. Today Proc.*, 5 (1) (2018) 184-192.

[17] P. K. Bajpai, K. Ram, L. K. Gahlot and V. K. Jha, Fabrication of glass/jute/epoxy composite based industrial safety helmet, *Mater. Today Proc.*, 5 (2) (2018) 8699-8706.

[18] M. Indra Reddy, M. Anil Kumar and C. Rama Bhadri Raju, Tensile and flexural properties of jute, pineapple leaf and glass fiber reinforced polymer matrix hybrid composites, *Mater. Today Proc.*, 5 (1) (2018) 458-462.

[19] M. K. Gupta and R. Singh, Flexural and dynamic mechanical analysis (DMA) of polylactic acid (PLA) coated sisal fibre reinforced polyester composite, *Mater. Today Proc.*, 5 (2) (2018) 6109-6114.

[20] H. Ullah, A. R. Harland and V. V. Silberschmidt, Experimental and numerical analysis of damage in woven gfrp composites under large-deflection bending, *Appl. Compos. Mater.*, 19 (5) (2012) 769-783.

[21] E. Soliman, U. Kandil and M. R. Taha, Improved strength and toughness of carbon woven fabric composites with functionalized MWCNTs, *Materials (Basel).*, 7 (6) (2014) 4640-4657.

[22] G. Gruber and S. Wartzack, Three point bending analyses of short fiber reinforced thermoplastics: A comparison, *SAS*

Tech., 12 (1) (2013) 1-8.

[23] M. Rafiquzzaman, M. Islam, H. Rahman, S. Talukdar and N. Hasan, Mechanical property evaluation of glass-jute fiber reinforced polymer composites, *Polym. Adv. Technol.*, 27 (10) (2016) 1308-1316.

[24] C. Dong, M. Kalantari and I. J. Davies, Robustness for unidirectional carbon/glass fibre reinforced hybrid epoxy composites under flexural loading, *Compos. Struct.*, 128 (2015) 354-362.

[25] L. Valarinho, J. Sena-Cruz, J. R. Correia and F. A. Branco, Numerical simulation of the flexural behaviour of composite glass-GFRP beams using smeared crack models, *Compos. Part B Eng.*, 110 (2017) 336-350.

[26] M. V. Ramana and S. Ramprasad, Experimental investigation on jute/carbon fibre reinforced epoxy based hybrid composites, *Mater. Today Proc.*, 4 (8) (2017) 8654-8664.

[27] A. P. Abhishek, B. S. K. Gowda, G. L. E. Prasad and R. Velmurugan, Probabilistic study of tensile and flexure properties of untreated jute fiber reinforced polyester composite, *Mater. Today Proc.*, 4 (10) (2017) 11050-11055.

[28] R. A. Braga and P. A. A. Magalhaes, Analysis of the mechanical and thermal properties of jute and glass fiber as reinforcement epoxy hybrid composites, *Mater. Sci. Eng. C*, 56 (2015) 269-273.

[29] H. Sezgin and O. B. Berkalp, The effect of hybridization on significant characteristics of jute/glass and jute/carbon-reinforced composites, *J. Ind. Text.*, 47 (3) (2017) 283-296.

[30] W. Hongxiao, D. Yugang, A. Dilimulati and Z. Xiaohui, Design optimization of CFRP stacking sequence using a multi-island genetic algorithms under low-velocity impact loads, *J. of Wuhan University of Technology-Mater. Sci. Ed.,* 32 (3) 720-725.

[31] E. Sevkat, B. Liaw and F. Delale, Drop-weight impact response of hybrid composites impacted by impactor of various geometries, *Mater. Des.*, 52 (2013) 67-77.

[32] F. Sarasini et al., Composites: Part B drop-weight impact behaviour of woven hybrid basalt - carbon / epoxy composites, *Compos. Part B*, 59 (2014) 204-220.

[33] A. Gopinath, M. Senthil Kumar and A. Elayaperumal, Experimental investigations on mechanical properties of jute fiber reinforced composites with polyester and epoxy resin matrices, *Procedia Eng.*, 97 (2014) 2052-2063.

[34] K. Sabeel Ahmed, S. Vijayarangan and A. Kumar, Low velocity impact damage characterization of woven jute—glass fabric reinforced isothalic polyester hybrid composites, *J. of Reinforced Plastics and Composites*, 26 (10) (2007) 959-976.

[35] B. S. Sugun and R. M. V. G. K. Rao, Low-velocity impact characterization of glass, carbon and kevlar composites using repeated drop tests, *J. of Reinforced Plastics and Composites*, 23 (15) (2004).

[36] S. Datta, A. V. Krishna and RMVGK Rao, Low velocity impact damage tolerance studies material, process and test parameters, *J. of Reinforced Plastics and Composites*, 23 (3) (2016).

[37] J. Zhang, B. L. Fox, D. Gao and A. W. Stevenson, Inspection of drop-weight impact damage in woven CFRP laminates fabricated by different processes, *J. of Composite Materials,* 43 (19) 1939-1946.

[38] ASTM D 7264, Standard test method for flexural properties of polymer matrix composite materials, *ASTM Stand.*, i (2007) 1-11.

[39] ASTM D7136, Standard test method for measuring the damage resistance of a fiber-reinforced polymer matrix composite to a drop-weight impact event, *ASTM Int. Des. D*, i (C) (2005) 1-16.

[40] E. Soliman, M. Al-Haik and M. R. Taha, On and off-axis tension behavior of fiber reinforced polymer composites incorporating multi-walled carbon nanotubes, *J. Compos. Mater.*, 46 (14) (2012) 1661-1675.

[41] D. Gay, S. V. Hao and S. W. Tsai, Ply properties, *Compos. Mater. Des. Appl.* (2003) 24.

Muhammad Ali Nasir is working as an Associate Professor and Director of Composite Materials & Smart Structures Laboratory, Department of Mechanical Engineering, University of Engineering & Technology, Taxila, Pakistan. He is doing research in the areas of advanced materials science, nanocomposites, smart structures, nanomaterials, fiber metal laminates, fractographic characterization of nano materials, materials characterization. E-mail: ali.nasir@uettaxila.edu.pk, Contact No: +92 3006026290.